PHILOSOPHICAL TRANSACTIONS A

royalsocietypublishing.org/rsta

CC BY

Research

Cite this article: Emberson L *et al.* 2026 Tropospheric Ozone Assessment Report II: Analysis of global ozone distribution and trends to assess vegetation impacts. *Phil. Trans. R. Soc. A* **384**: 20250270.
https://doi.org/10.1098/rsta.2025.0270

Received: 31 December 2025
Accepted: 2 July 2026

One contribution of 8 to a theme issue 'Tropospheric Ozone Assessment Report II'.

Subject Areas:
atmospheric science, atmospheric chemistry, biogeochemistry, ecosystem, climatology, geophysics

Keywords:
tropospheric ozone, atmospheric composition, vegetation damage, metrics, trends, air quality policy

Author for correspondence:
Lisa Emberson
e-mail: l.emberson@york.ac.uk

Supplementary material is available online at https://doi.org/10.6084/m9.figshare.c.8631039.

THE ROYAL SOCIETY PUBLISHING

Tropospheric Ozone Assessment Report II: Analysis of global ozone distribution and trends to assess vegetation impacts

Lisa Emberson[1], Tamara Emmerichs[2], Pierluigi Guaita[3,4], Abdulla A. Mamun[5], Felicity Hayes[6], Sabine Schroeder[7], Anthony Y. H. Wong[8], Nathan Booth[1], Riccardo Marzuoli[3], Giacomo Gerosa[3], Martin Schultz[7,9], Min Huang[10] and Leiming Zhang[5]

[1]Department of Environment and Geography, University of York, York, UK
[2]Max Planck Institute for Meteorology, Hamburg, Germany
[3]Department of Mathematics and Physics, Catholic University of the Sacred Heart, Brescia, Italy
[4]Department of Applied Computational Mathematics and Statistics, University of Notre Dame, Notre Dame, Indiana, USA
[5]Environment and Climate Change Canada, Toronto, Canada
[6]UK Centre for Ecology & Hydrology
[7]Jülich Supercomputing Centre, Forschungszentrum Jülich, Germany
[8]Massachusetts Institute of Technology, Cambridge, MA, USA
[9]Department of Computer Science, University of Cologne, Germany
[10]University of Maryland, College Park, MD, USA

LE, 0000-0003-3463-0054; PG, 0000-0002-5970-8113; AAM, 0000-0002-8142-1178; FH, 0000-0002-1037-5725; AYHW, 0000-0001-6386-3063; RM, 0000-0001-5946-9530; MS, 0000-0003-3455-774X; MH, 0000-0001-9361-0198

We use the TOAR-II database to explore vegetation risk from surface ozone when characterized by different concentration- and flux-based metrics for three crop species (wheat, rice and soybean) and three

© 2026 The Authors. Published by the Royal Society under the terms of the Creative Commons Attribution License http://creativecommons.org/licenses/by/4.0/, which permits unrestricted use, provided the original author and source are credited.

Downloaded from royalsocietypublishing.org/rsta/article-pdf/doi/10.1098/rsta.2025.0270/6174187/rsta.2025.0270.pdf
by Univ. of Maryland user
on 30 October 2026

forest species (beech and a sensitive and tolerant tropical tree species). From analysis of up to 3363 sites of present-day (2016–2021) ozone levels, we find some differences between metrics with 64% and 90% of sites exceeding critical levels for irrigated wheat and 85% and 79% for beech for concentration- and flux-based metrics, respectively. Overall, the flux-based metric tends to suggest higher levels of risk. Metrics estimate similar global trends at up to 3242 sites for the period 2005 to 2021 with between 14% and 40% of sites showing statistically significant decreasing trends, which are most prevalent in North America (NAM), followed by Europe (EUR). We use the flux-based metric and literature-derived flux-response relationships to estimate average relative yield losses of 4.9% for irrigated wheat, and losses of relative gross annual increment of 14.3%, 19.8% and 5.9% for beech, sensitive and tolerant tropical tree species, respectively. Results for soybean and rice are inconclusive. Future research should extend the TOAR database in Asia (AS), Africa and Latin America and improve flux-based methodologies.

This article is part of the theme issue 'Tropospheric Ozone Assessment Report II'.

1. Introduction

A wealth of observational and experimental evidence exists describing the impacts of ground-level ozone on crops, forests and ecosystems [1]. Although this evidence derives from a relatively small number of individual study sites, these cover important global regions which have experienced past levels of elevated ozone, predominantly North America (NAM), Europe (EUR) and Asia (AS) [1], but also a limited number of studies in South America [2,3]. Ozone impacts on agricultural crops have been summarized in several review papers (e.g. [4–6]) with a reasonably large number of different crop species having been investigated. Such studies demonstrate the potential for ozone to impact food production with more recent findings showing that ozone can also affect the nutritional yield of crops [7,8]. This highlights the potential role of this air pollutant to negatively affect food security [9]. For forests, a large body of evidence has also been accumulated over the past few decades describing the impacts of ozone on a variety of tree species, primarily in NAM and EUR [10,11] and increasingly in AS [12]. Such studies are useful in demonstrating the potential for ozone to impact tree growth and productivity, which is becoming increasingly important owing to the potential impact of ozone on carbon sequestration [13,14].

To allow assessment of the potential ozone impacts on food supply, forest productivity and carbon sequestration across broader geographical regions requires modelling the risk of ozone damage. There are several modelling approaches with the most common being ozone risk assessments that use dose-response relationships (DRRs) to relate ozone exposure either to an exceedance of an air quality guideline or quantification of actual damage [1]. Over the past few decades, several different ozone exposure metrics have been developed to support national, regional and global assessments of ozone impacts to vegetation. These metrics have evolved from concentration-based indices that have focused on mean daylight growing season averages (i.e. M7 and M12) or weighted metrics that emphasize higher concentrations accumulated over the growing season (i.e. W126 and AOT40). Further details of these concentration-based metrics are given in the previous TOAR-I vegetation assessment [15], which explored trends in how these concentration-based metrics changed over time by global region.

Over the past two decades, flux-based metrics (i.e. PODy) have been developed, which consider cumulative stomatal ozone uptake (rather than ozone concentration) over the growing season. These metrics allow for the fact that decoupling can occur between ozone concentration and ozone uptake by vegetation when high temperatures, low atmospheric humidity and soil water stress can limit stomatal conductance (g_{sto}), the primary pathway by which ozone enters plant leaves and causes damage. These metrics were found to be more biologically relevant [16], which has led to their adoption for use within the United Nations Economic Commission for Europe (UNECE)'s Convention on Long-range Transboundary Air Pollution (CLRTAP). Flux-based

Downloaded from royalsocietypublishing.org/rsta/article-pdf/doi/10.1098/rsta.2025.0270/6174187/rsta.2025.0270.pdf
by Univ. of Maryland user
on 30 October 2026

critical levels have also been derived in EUR to determine regions of critical level exceedances of ozone exposure for crops, trees and grasslands [17,18].

Regional and global assessments based on these various risk assessment methods have indicated that ozone pollution causes significant impacts on crop losses and forest growth worldwide [1]. However, a crop study by Tai *et al.* [19] highlighted how the choice of metric played a substantial role in determining the magnitude of estimated yield losses; wheat and soybean generally showed greater losses, though with large variability depending on the metric used. For these species, AOT40 estimated a far greater yield loss than M7/M12 for wheat (at approx. 13% and 2%, respectively, as an aggregated global yield loss), whereas for soybean, M7/M12 estimated a greater yield loss than AOT40 (at approx. 14% and 6%, respectively). By contrast, rice and maize generally showed lower yield losses (up to 5%) and hence less variability between metrics.

In addition, very few studies have evaluated the accuracy of modelled estimates of ozone risk. Crucially, the few studies that do exist find that the flux-based ozone metric provides a better estimate of the spatial distribution of risk than the AOT40 concentration-based metric (i.e. of visible injury and growth reduction to clover [20] and biomass reductions in young trees [21]). This is generally attributed to meteorological or environmental conditions (i.e. high atmospheric and soil water deficits [20]) that can decouple higher ozone concentrations from ozone uptake and hence ozone damage. It is therefore important to understand how different metrics quantify risk, both across geographical regions (where environmental factors known to influence plant sensitivity to ozone may vary [22]) as well as over time (where changes in ozone exposure regime may be influenced by emission reductions). Together, these effects can result in different metrics leading to different conclusions about the effect of changes in the drivers of ozone variability (e.g. precursor emissions) on vegetation exposure and damage [23].

The previous TOAR-I vegetation assessment paper [15] explored geographical distribution and trends in the magnitude of concentration-based metrics from 2000 to 2014. To build on this work, a concerted effort has been made over the past few years to enable the estimation of flux-based metrics within the TOAR database (https://toar-data.org/) by embedding a version of the DO_3SE model, used within the CLRTAP to estimate ozone deposition and stomatal ozone flux, culminating in webDO3SE [24]. This webDO3SE model calculates ozone uptake using an ozone deposition scheme that comprises a sunlit and shaded big-leaf [25] and estimates stomatal ozone flux according to a multiplicative, Jarvis-type, g_{sto} model [26–28]. The model is parametrized for a broad range of vegetation types and can be run for defined growth periods, allowing calculation of ozone flux for individual TOAR database monitoring stations. Species-specific ozone flux estimates from WebDO3SE can be combined with vegetation-specific dose-response functions to calculate annual site-specific losses in productivity for a range of species. Calculations of spatial distribution and temporal trends of ozone damage can also be estimated at multiple sites and thus help identify global regions with current and emerging threats to vegetation from tropospheric ozone pollution. The TOAR database provides a unique opportunity to make such comparisons for many stations over the extended period for which TOAR ozone data have been collected. Here, we focus on the last two decades (specifically 2005 to 2021) using approaches described in §2. As such, the overall aim of this paper is to identify those global regions with current and emerging threats from ozone in relation to vegetation impacts and to showcase the webDO3SE tool and its potential contribution to inform policy making over different time horizons (i.e. near-term air quality guideline-based risk assessments versus medium to longer-term assessments of different emission pathways).

2. Methods

The key differences between concentration- and flux-based metrics in relation to webDO3SE are described in figure 1. WebDO3SE calculates total ozone deposition to the canopy, while the PODy metric represents cumulative stomatal ozone uptake to a representative leaf of the upper canopy

Downloaded from royalsocietypublishing.org/rsta/article-pdf/doi/10.1098/rsta.2025.0270/6174187/rsta.2025.0270.pdf
by Univ. of Maryland user
on 30 October 2026

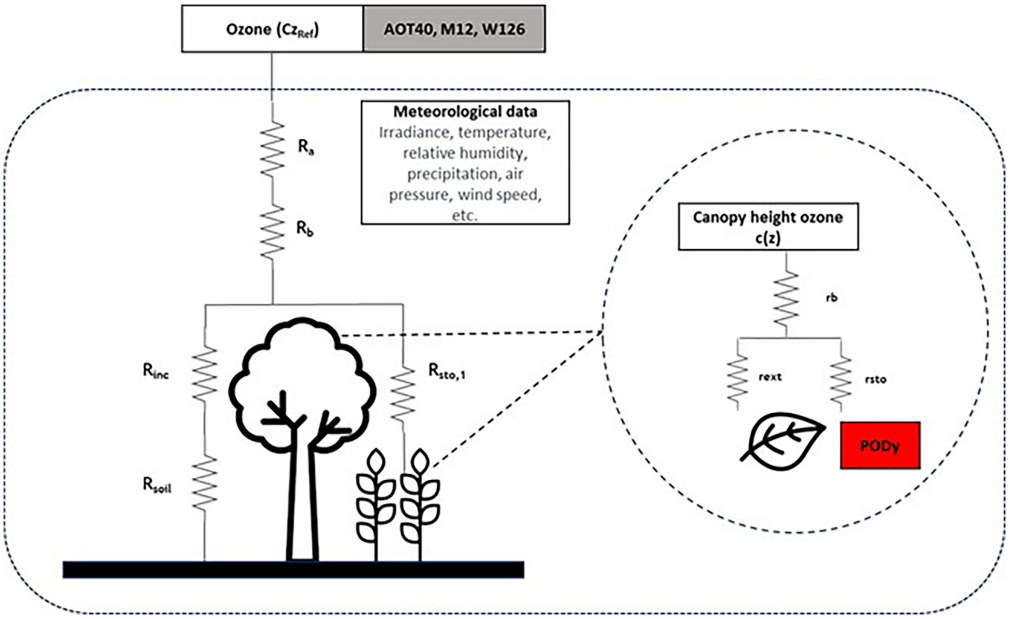

Figure 1. Schematic of ozone metrics explaining the difference in the concentration-based (M12, AOT40 and W126) versus flux-based (PODy) metrics in relation to the DO_3SE deposition scheme. The round-edged box denotes the components of the DO_3SE model, and the circle denotes the components of the DO_3SE model that are used to calculate the leaf-level PODy metric. Where Cz_{Ref} is the ozone concentration at a reference height above the canopy, R_a, R_b, R_{inc}, R_{soil} and R_{sto} are canopy-level atmospheric, boundary layer, within-canopy and soil resistances to ozone transfer, *c(z)* is the ozone concentration at the top of the canopy, r_b, r_{ext} and r_{sto} are leaf-level resistances to boundary layer, cuticle and stomatal transfer to ozone. Further clarification of the distinction between *R* and *r* terms (denoting canopy- and leaf-level, respectively) can be found in [29].

(here depicted for both a tree and a crop; see also [29] for details of the distinction between canopy- and leaf-level resistances used in the DO_3SE scheme). Ideally, concentration-based metrics would be calculated for canopy height ozone concentrations, but this is not always the case since application of a deposition scheme is required to derive canopy height concentrations if measurements are taken at some height above the canopy. Flux-based metrics were excluded from the previous TOAR-I vegetation assessment [15] since the meteorological data required to estimate the metric were not readily available. The recent inclusion within the TOAR database of ERA5 meteorological data (supplementary material, table S1) potentially allows PODy estimation at all 24347 TOAR sites around the world for periods between 1974 and 2023. In this study, ERA5 data have been used at all sites that meet our site selection criteria described in §2c. One key limitation of the TOAR data is the unavailability of measurement height data (i.e. what height above ground are the ozone concentrations measured). To overcome this limitation, we assume all ozone concentrations are measured at 3 m but explore the implications of this assumption in the sensitivity analysis described in §4. The fact that TOAR data are harmonized, synthesized and quality controlled to minimize uncertainty [30,31] and freely and openly available through a graphical user interface and a representational state transfer interface (https://toar-data.fz-juelich.de/api/v2/, last access: 13 August 2025) enables end users to perform similar analyses to those described in this study.

(a) Species selection, distribution and growing season

We calculated metrics (M12, AOT40, W126 and PODy) for three staple crops and three forest tree species. Wheat (*Triticum aestivum*), soybean (*Glycine max*) and rice (*Oryza sativa*) were selected

Downloaded from royalsocietypublishing.org/rsta/article-pdf/doi/10.1098/rsta.2025.0270/6174187/rsta.2025.0270.pdf
by Univ. of Maryland user
on 30 October 2026

owing to their broad global coverage (with 220, 168 and 136 Mha, respectively, in 2023 [32]), known sensitivity to ozone [33,34] and the availability of established PODy flux-response relationships with associated g_{sto} parametrizations. Wheat and rice were also investigated in the TOAR-I vegetation assessment [15], allowing a comparison of trends in concentration-based metrics. We investigate two types of forest tree species, temperate/boreal deciduous and tropical. Beech (*Fagus sylvatica*) was selected to represent a temperate/boreal deciduous tree species owing to its ozone sensitivity and because deciduous species are considered more sensitive to ozone than coniferous species [35,36]. We used the g_{sto} parametrization for continental beech described in the CLRTAP Mapping Manual [37] and the PODy flux-response relationship for this plant functional type [35]. Far less is known about tropical tree species responses to ozone, and we based our species selection and g_{sto} parametrization on a recent study by Cheesman *et al.* [14], who investigated ozone effects on biomass growth across a wide range of tropical deciduous and evergreen species. We selected two tropical tree species that provide a range of ozone-sensitive responses. We used *Inga edulis* as a moderately ozone-sensitive tropical species and *Calophyllum inophyllum* as a less sensitive species to provide a range of the estimated potential damage across the tropics. These two species were also selected because together they broadly cover the global tropics, with *I. edulis* most widely distributed in South America and *C. inophyllum* having a good distribution in Africa, Southeast AS and Australia. The parametrizations required by WebDO3SE for all species are summarized in table S2 in the supplementary material.

We updated the TOAR database metadata to define crop distribution and growing season. Crop distribution data are taken from the Food and Agriculture Organization (FAO) Global Agro-Ecological Zones (GAEZ) [38] database, compiled as crop production data so that the absence of crop production identifies sites where a crop is not grown. The FAO GAEZ data define spring and winter wheat, rice and soybean. We updated the TOAR-II Analysis Service to use the maturity dates from the Global Gridded Crop Model Intercomparison (GGCMI) Phase 3 crop calendar [39] to define the 'end of growing season' (EGS) for each crop species. We use the EGS since this can be defined with more accuracy than crop emergence or anthesis within the GGCMI Phase 3 data [39]. We compare these new growing season periods with those used in the previous TOAR-I vegetation assessment in table S3 in the supplementary material and show the spatial distribution of GGCMI-defined EGS in fig. S2 in the supplementary material. We find reasonable consistency between both GGCMI and TOAR-I data, especially when wheat type is considered (supplementary material, §2c). Since the GGCMI Phase 3 calendar is considered one of the most robust, state-of-the-art tools for global-scale modelling of crop impacts, we make use of this calendar in this study while recognizing limitations such as the static nature of growing periods (unrelated to temperature), as well as spatial limitations related to data gaps [39]. For forests, we use the metadata associated with the ozone monitoring sites in the TOAR-II Analysis Service to define global climate biome categories to identify tropical and boreal/temperate forest species distributions as used previously in the TOAR-I vegetation assessment [15]. This is achieved by selecting any of the TOAR land cover categories that include a 'broad-leaved' tree category (including mosaic tree) and are outside of the latitude bands 20°N and 20°S. The distribution of tropical trees is defined by the TOAR database metadata as any tree category that falls within the latitude bands 20°N and 20°S.

(b) Metric calculation

(i) Concentration-based metrics

Concentration-based metrics (M12, W126 and AOT40) were estimated within the TOAR database (https://toar-data.org/) using the algorithms described previously in the TOAR-I vegetation assessment [15], which are detailed in §S1 in the supplementary material. These concentration-based indices were calculated over 92 days for all three crop species. For beech trees, the metrics are averaged over a growing season defined by a fixed six-month growing season [37], and for tropical trees, they are averaged for the entire year.

Downloaded from royalsocietypublishing.org/rsta/article-pdf/doi/10.1098/rsta.2025.0270/6174187/rsta.2025.0270.pdf
by Univ. of Maryland user
on 30 October 2026

(ii) Flux-based metric (PODy)

The flux-based metric PODy was estimated using WebDO3SE as described in §S2 in the supplementary material. The estimate of PODy requires meteorological data (irradiance, air temperature, relative humidity, precipitation, air pressure and wind speed), which have been extracted from the fifth generation of ECMWF reanalysis (ERA5) for global climate [40] and incorporated within the TOAR database so that it can be directly used by WebDO3SE (see supplementary material, table S1 for a full list of variables). The PODy accumulation periods for crops align the end of the PODy accumulation period with the EGS (the maturity date given by the GGCMI crop calendar [39]), with starts fixed at 45, 60 and 92 days earlier than the EGS (thereby allowing for differences in the timing of the growing season by location) for wheat, rice and soybean, respectively. This length of accumulation period is defined by the associated crop-specific flux-response relationship (and the period of ozone fumigation and crop sensitivity for which the relationship was developed—see supplementary material, table S8). We assume that all crops are irrigated. This is a simplification that follows a precautionary approach, since irrigation would enhance ozone uptake owing to the removal of soil water stress limiting g_{sto} [41]. This approach is considered appropriate given the difficulties in identifying the area under irrigation and irrigation use throughout the growing season by global datasets. For example, a recent study estimated an 18% larger irrigated area than that identified using existing approaches based on statistical data, with the largest deviations occurring in AS (particularly India and the People's Republic of China) [42]. For forests, the PODy metric is accumulated for the same period as defined for the entire growing season [37]. For beech, we assume a six-month growing season which runs between 1 April and 30 September in the Northern Hemisphere and 1 October and 31 March in the Southern Hemisphere. We acknowledge that this will create larger differences (flipped growing seasons) for any deciduous species found closer to the equator, but only very few beech sites fell into this category, so this does not affect the current analysis. For the two parametrizations of evergreen tropical trees (*I. edulis and C. inophyllum*), we used a year-round (12-month) growing season and PODy accumulation period.

(c) Selection of TOAR database sites

We use average metric values for each site from 2016 to 2021 to characterize the present-day ozone concentrations, while we consider values over the historical period of 2005–2021 to investigate trends in ozone metrics. We identified the TOAR database sites to use in these analyses according to the following three key criteria. First, all 'rural' and/or 'background' stations in the TOAR database were considered, while urban stations were included if they showed that agricultural production for the relevant crops (wheat, rice and soybean) was more than 0.099 thousand tonnes per year. Second, to ensure the data represent a robust time series of within-year or growing season data, we only used sites that have a data capture of greater than or equal to 75% for daylight hourly ozone concentrations over the averaging time or accumulation period of each metric. Finally, we consider the length of the time series, the 'present' period (2016–2021), require all 6 years of data to conform to our data capture criteria. The 'historical' period required at least 12 years of data starting no later than 2007 and ending no earlier than 2019 (for 2005–2021). The number of sites that meet these criteria by species and metric for each period is listed in table S4 in the supplementary material. We also added additional modelled ozone data to extend the geographical coverage of our assessment into data-poor ozone observation regions. This extension used data from the TRopospheric Ozone and its Precursors from Earth System Sounding (TROPESS) Chemical Reanalysis Surface O3 2-Hourly 2-dimensional Product V1 provided at GES DISC, which has ozone data availability from 2005 to 2021. The TROPESS reanalysis data come from a tropospheric chemical reanalysis product developed from assimilation of updated satellite measurements of ozone into the MIROC-CHASER chemistry transport model [43], the uncertainty of which has been discussed in [44]. We used these data to provide ozone concentration data for 'Open AQ' TOAR database sites since these sites already have ERA5 meteorological data collated.

Downloaded from royalsocietypublishing.org/rsta/article-pdf/doi/10.1098/rsta.2025.0270/6174187/rsta.2025.0270.pdf
by Univ. of Maryland user
on 30 October 2026

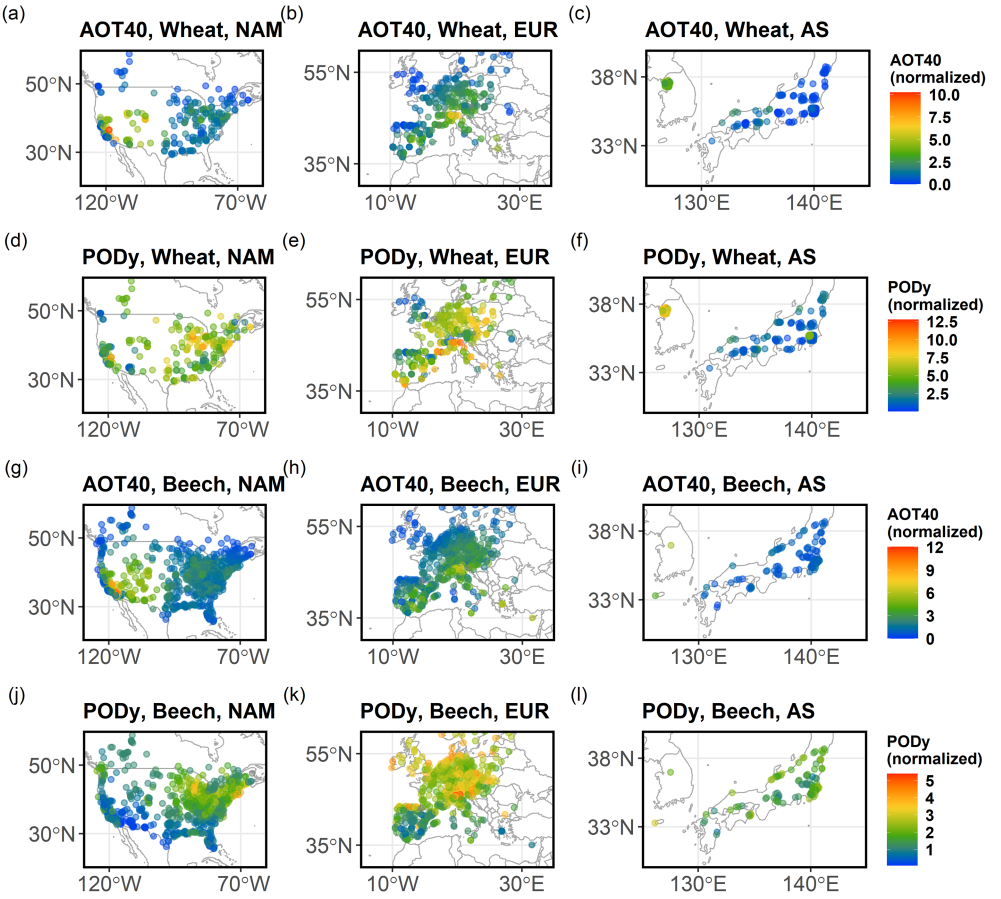

Figure 2. Comparison of the regional (NAM, EUR and AS) distribution of the normalized mean AOT40 (a–c and g–i) and PODy (d–f and j–l) values for 2016–2021, for wheat (a–f) and beech (g–l).

3. Results

(a) Present-day metrics

Overall, up to 3363 sites met the criteria for inclusion for metric analysis with PODy having the largest number of sites owing to the shorter growing season required by some crops for metric calculation. The PODy sites split out into crops (wheat (828), soybean (477), rice (365)) and forest trees (beech (1662) and tropical (31)) for the present-day (2016–2021) analysis period. Absolute values for all metrics (M12, AOT40, W126 and PODy) are shown in global maps in figs. S3 and S4 in the supplementary material. It is useful to compare the magnitude and spatial distribution of the relative risk indicated by the metrics, which is achieved by normalizing the metrics, either using a critical level or the metric value at which relative yield loss (crops) or biomass loss (trees) is equal to 5% (see supplementary material, table S5—referred to as the nominal critical level). Here, we focus on two vegetation types (wheat and beech) and explore three different regions: NAM, EUR and AS and compare the AOT40 and PODy metrics, since critical levels for these two metrics and species are defined by CLRTAP [37]; the results are shown in figure 2. Results for all metrics are also summarized in the table S6 in the supplementary material, and for AOT40, M12 and PODy for wheat, rice, soybean and beech in the three main regions (AS, EUR and NAM) in fig. S5 in the supplementary material.

Downloaded from royalsocietypublishing.org/rsta/article-pdf/doi/10.1098/rsta.2025.0270/6174187/rsta.2025.0270.pdf
by Univ. of Maryland user
on 30 October 2026

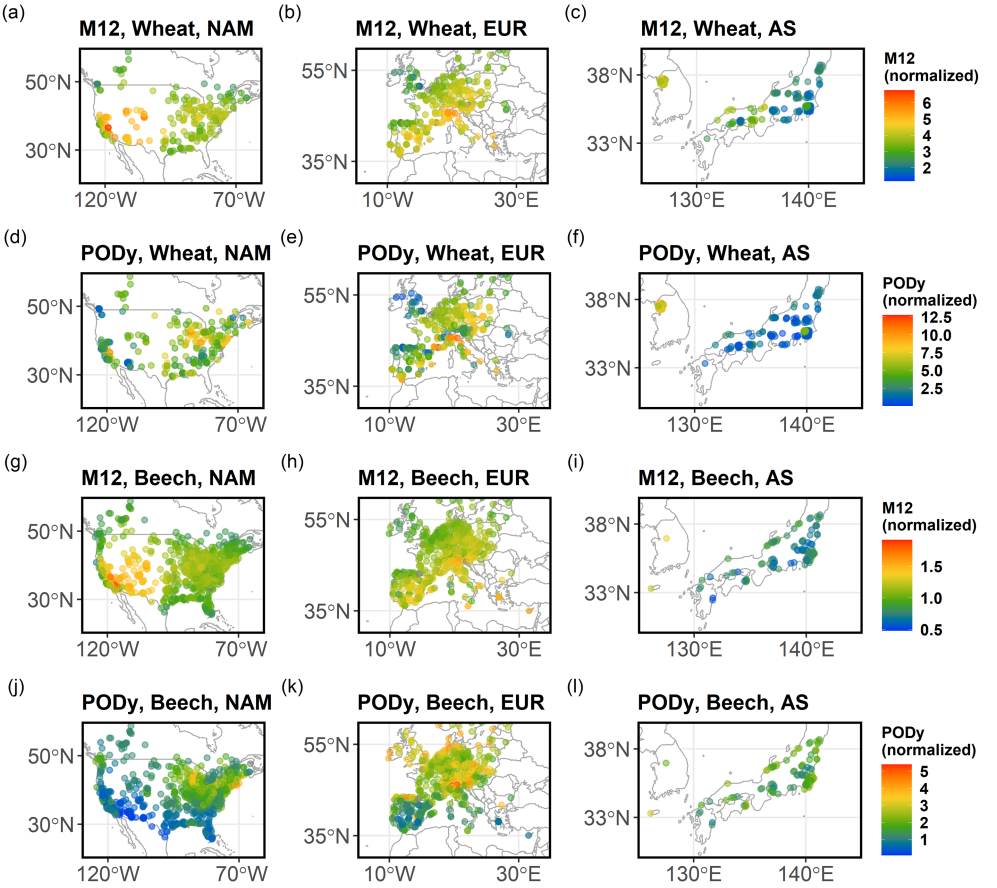

Figure 3. Comparison of the regional (NAM, EUR and AS) distribution of the normalized mean M12 (a–c and g–i) and PODy (d–f and j–l) values for 2016–2021, for wheat (a–f) and beech (g–l).

Globally, we find that for wheat, 64% and 90% of sites exceed the critical level for AOT40 and PODy, respectively. This pattern of higher numbers of exceedances with the PODy compared to the AOT40 metric is consistent across all three global regions. For beech trees, the results using different metrics are more similar, with 85% and 79% of sites showing exceedance for AOT40 and PODy, respectively. However, substantially more sites show exceedance in EUR and AS with PODy, while more sites in the NAM region show exceedance with AOT40. Although the M12 metric is not used for critical level exceedance, this metric shows the highest risk across all crops and regions (with close to 100% of sites exceeded except for rice in AS where only 38% of sites were exceeded, though this is still far higher than the AOT40 estimated risk). The M12 metric suggests similar risk for beech across all regions except for lower (only 3% of sites in exceedance) in AS, where both AOT40 and PODy suggest far higher risk (35% and 96% of sites in exceedance, respectively).

We also explored the scale of risk suggested by different metrics (i.e. by how much the nominal critical levels are exceeded) and focused on M12 and PODy to use a concentration-based metric that also included lower-end ozone concentrations. First, figure 3 highlights the disparities in the number of sites for each of the three regions. Overall, there are more sites in NAM (up to 1362), slightly fewer sites in EUR (up to 1125) and substantially fewer sites in AS (840 for M12 and only 591 for PODy). Perhaps more importantly, the AS sites are only located in two countries (Japan and the Republic of Korea), making robust comparisons of metrics challenging in AS. For wheat, the spatial distribution of risk estimated by M12 and PODy is similar, though with moderately

Downloaded from royalsocietypublishing.org/rsta/article-pdf/doi/10.1098/rsta.2025.0270/6174187/rsta.2025.0270.pdf
by Univ. of Maryland user
on 30 October 2026

higher risk estimated in Western NAM. For beech, the pattern of difference is starker and more widespread with substantially higher risk estimated using the M12 metric in Mid- and Western-NAM and Southern EUR. Figure S6 in the supplementary material shows that for soybean, M12 suggests a substantially higher risk in NAM and EUR, while the risk in AS is similar when using either metric. The ozone risk to rice estimated by PODy is minimal, while M12 suggests some ozone risk to rice across all regions, though in AS, this risk occurs predominantly in the Republic of Korea (not Japan). Figures S7 and S8 in the supplementary material show normalized exceedance for all species for AOT40 and W126 for comparison. Figure S9 in the supplementary material shows the results for tropical forests, though only 31 sites met the criteria for analysis for concentration- and flux-based metrics. Globally, 74% and 61% of sites exceeded nominal concentration-based critical levels (AOT40 and M12), and 100% of sites exceeded the PODy critical level using the sensitive tropical tree DRR. However, since critical levels have not been officially defined for tropical trees, these results are only indicative.

Frequency plots showing the percentage of sites by each region that fall into value categories of each ozone metric are shown for all crop species and beech in figs. S10 and S11 in the supplementary material. Figure S10 in the supplementary material shows that for wheat, both M12 and PODy show a similar distribution between the three global regions with the highest values in NAM, closely followed by EUR; AS does not follow a normal distribution owing to many sites with low metric values. For rice and soybean, the M12 metrics follow a normal distribution, again apart from AS for which there are many sites with lower values. This non-normal distribution is found for PODy in all regions, but particularly in NAM and EUR, while AS has instances of some higher values. Finally, beech has a similar distribution for both M12 and PODy metrics across all three global regions, though AS values tend to be far lower for both PODy and M12. AOT40 and W126 metrics have similar patterns across all species and regions, as would be expected given that these are both accumulative indices that weight higher concentrations (supplementary material, fig. S11).

(b) Historical trends in metrics

We explore trends between the years 2005–2021 using both the concentration- and flux-based metrics to assess trends by region (NAM, EUR and AS) and by species (wheat, rice, soybean and beech). Our trend analysis uses Mann–Kendall methods (see supplementary material, §S3 for details). Only species with 10 or more sites that fulfil the data availability criteria are considered for discussion. Increasing and decreasing trends are considered for $p < 0.05$. Table S7 in the supplementary material summarizes all trend results by metric, species and region. Overall, for the three crops and beech, we find that globally there are more sites with statistically significant decreasing trends (30%, 14%, 39% and 40%, for M12, PODy, AOT40 and W126, respectively) than those with increasing trends (where only 9%, 4%, 6% and 5% of sites have statistically significant increasing trends, respectively). There is a substantially larger proportion of sites with statistically significant decreasing trends in NAM than in EUR (56%, 23%, 65% and 66% of sites for NAM compared to 10%, 7%, 13% and 16% of sites for EUR), again for M12, PODy, AOT40 and W126, respectively. For the AS region, the picture is more mixed with similar numbers of sites showing both an increase and a decrease in trends. AOT40 and W126 both suggest a decreasing trend (both metrics have 29% of sites showing a decrease and 18% of sites showing an increase). For M12 and PODy, sites with increasing trends (23% and 14%, respectively) are more prevalent than those with decreasing trends (16% and 10%, respectively).

For wheat, figure 4 shows that both M12 and PODy show a decreasing ozone risk in NAM of 50% (M12) and 40% (PODy) of sites with largely no change at the remaining sites. Both metrics suggest predominantly no change in EUR, although the M12 metric has a few sites showing both a decrease and an increase (7% and 6%, respectively). These results can be deemed relatively robust with 323 EUR sites and 257 NAM sites for M12 and 315 EUR and 258 NAM sites for PODy included in the analysis. The AS region has 226 and 223 sites for M12 and PODy, respectively,

Downloaded from royalsocietypublishing.org/rsta/article-pdf/doi/10.1098/rsta.2025.0270/6174187/rsta.2025.0270.pdf
by Univ. of Maryland user
on 30 October 2026

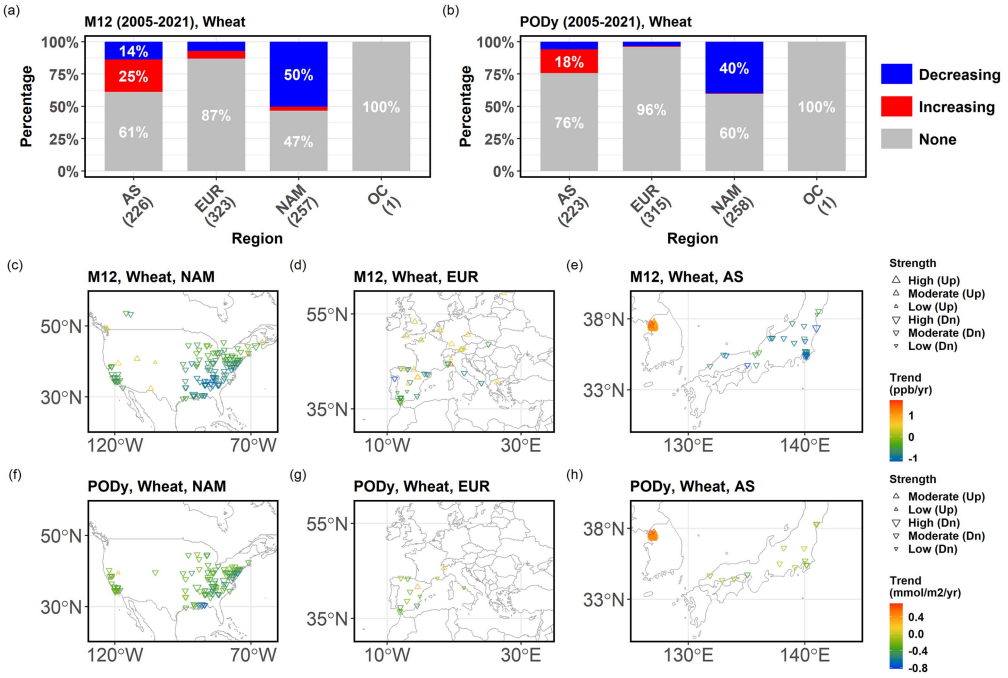

Figure 4. Statistical trends (bar charts, a–b) and spatial distribution (maps, c–h) of trends between 2005–2021 for the M12 and PODy metric by global region (AS, EUR and NAM) for wheat. For the bar charts (a and b), significant trends ($p < 0.05$) with high ($|\tau| >= 0.7$), moderate ($0.4 <= |\tau| < 0.7$) and low ($0.1 <= |\tau| < 0.4$) strengths are combined, and the remaining trends (i.e. trends with significance $p >= 0.05$ and/or $|\tau| < 0.1$) are grouped as 'none'. The total number of sites that fulfil the data availability criteria is shown in parentheses along the x-axis in (a) and (b).

included in the analysis, but those sites which showed either increasing or decreasing trends were all located in the Republic of Korea or Japan. Both metrics overall show an increasing trend (25% for M12 and 18% for PODy); however, these trends depend on location with all increases located in the Republic of Korea and the decreases (14% for M12 and 6% for PODy) located in Japan. As such, a much broader spatial distribution of sites is required in AS to make any robust statements as to the trends in ozone exposure by metric. For beech trees, figure 5 shows differences between M12 and PODy in the extent of trends in ozone risk over the period 2005–2021. M12 has more sites showing a decreasing trend with 58% in NAM, 11% in EUR and 24% in AS, and most of the remaining sites show no change. By contrast, PODy shows fewer sites with a decreasing trend (12%, 10% and 17% of sites for NAM, EUR and AS, respectively), the remaining sites also predominantly show no change. The region identified as having the greatest decreasing trend is also dependent upon metric selection with M12 estimating the greatest decrease in NAM (at 58% of sites), while the PODy metric shows AS to have the greatest decrease with 17% of sites trending downwards.

The results for soybean (supplementary material, table S7 and fig. S12) are less robust since only the NAM region has a substantial number of sites included in the analysis (175 for both M12 and PODy). Both metrics showed a substantial proportion (59% for M12 and 50% for PODy) of these sites showing a decreasing trend, while the remainder showed predominantly no change. For the EUR region (including 49 and 47 sites for M12 and PODy, respectively), both metrics predominantly suggest no change though M12 has 3% and 4% of sites showing a decrease and increase, respectively. There are 241 and 239 sites in AS for M12 and PODy analysis, respectively, but again, these sites showing significant trends are limited to the Republic of Korea and Japan; similar to wheat, both metrics for soybean show an increasing trend in the Republic of Korea and a decreasing trend in Japan, though the latter is not as strong for PODy as it is for M12. Finally, rice

Downloaded from royalsocietypublishing.org/rsta/article-pdf/doi/10.1098/rsta.2025.0270/6174187/rsta.2025.0270.pdf
by Univ. of Maryland user
on 30 October 2026

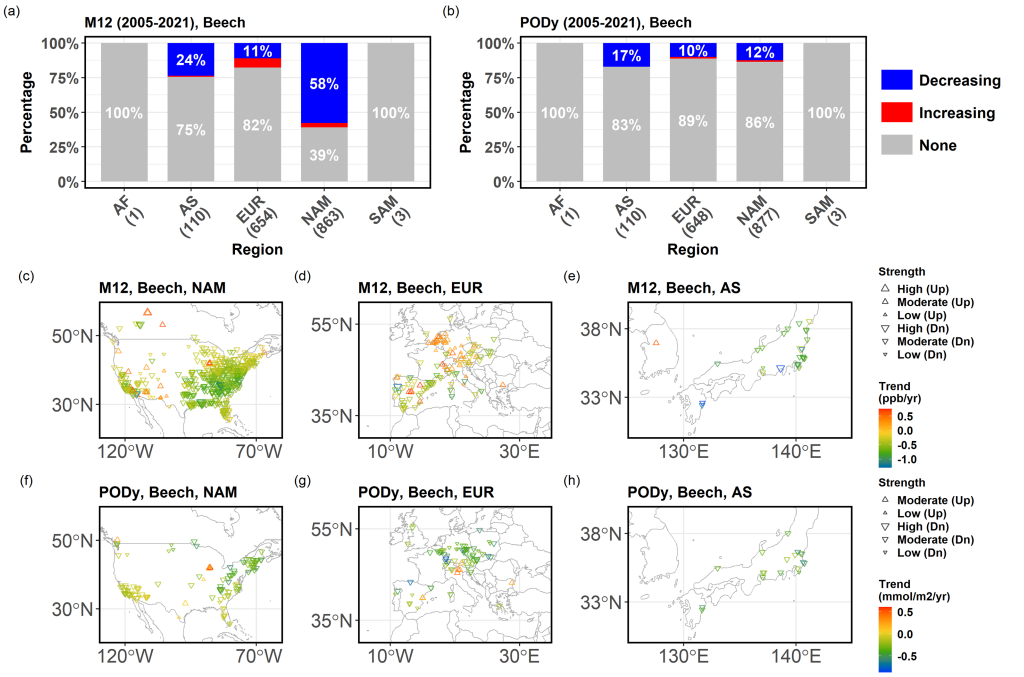

Figure 5. Statistical trends (bar charts, a–b) and spatial distribution (maps, c–h) of trends between 2005–2021 for the M12 and PODy metric by global region Africa (AF), AS, EUR, NAM and South America (SAM) for beech trees. For the bar charts (a and b), significant trends ($p < 0.05$) with high ($|\tau| >= 0.7$), moderate ($0.4 <= |\tau| < 0.7$) and low ($0.1 <= |\tau| < 0.4$) strengths are combined, and the remaining trends (i.e. trends with significance $p >= 0.05$ and/or $|\tau| < 0.1$) are grouped as 'none'. The total number of sites that fulfil the data availability criteria is shown in parentheses along the x-axis in (a) and (b).

(supplementary material, table S7 and fig. S13) has the fewest number of sites that meet the trend analysis criteria of any species with only 42 in NAM and up to 70 in EUR. There are many sites in AS (up to 243), but again with very limited spatial distribution of sites with significant trends. The PODy metric suggests a decrease in NAM (at 21% of sites) and both a decrease (at 15% of sites) and an increase (at 13% of sites) in AS. By contrast, M12 suggests a more substantial decreasing trend of 48% and 14% of sites in NAM and EUR, but also shows some increasing trends in NAM (at 14% of sites) and particularly in AS (at 26% of sites compared to only 14% of sites showing a decrease in this region). Regional trends for AOT40 and W126 for wheat, rice, soybean and beech are given in figs. S14–S17 in the supplementary material; global trends for each species and metric are also given in figs. S18–S21 in the supplementary material.

One of the main reasons why metrics may give different trend results is the composition of the ozone distribution (i.e. how many hours over the metric averaging or accumulation period are made up of ozone concentrations of different magnitudes). To investigate this, we show how ozone concentrations (divided into bins of 10 ppb increments) contribute to the overall metric values between 2005 and 2021. Figure 6 shows that for beech trees in EUR (which had a good number of sites at 648 for both M12 and PODy, respectively), the contribution of ozone concentrations to the metrics was very similar for each year over the entire period with concentrations within the range of 30 to 60 ppb making up the bulk of the metric contribution. Similar results were found for NAM and AS for beech tree species.

By contrast, figure 7 shows the ozone concentration profile for soybean in NAM, where 175 sites for both M12 and PODy are included in the analysis. Here, the ozone concentrations that contribute to the metrics are very different, predominantly ranging from 20 to 50 ppb for M12. By contrast, PODy is mostly made up of higher ozone concentrations reaching above 90 ppb with concentrations between 60 and 80 ppb often making up about 20% of the metric contribution in

Downloaded from royalsocietypublishing.org/rsta/article-pdf/doi/10.1098/rsta.2025.0270/6174187/rsta.2025.0270.pdf
by Univ. of Maryland user
on 30 October 2026

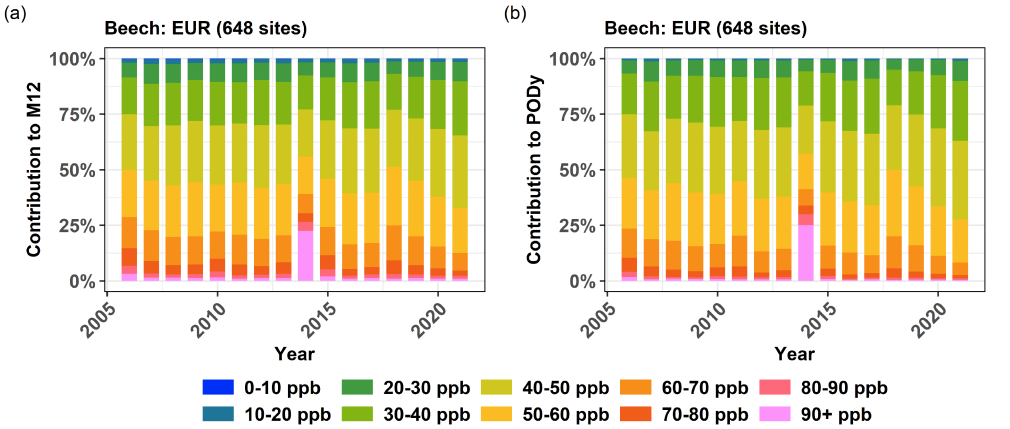

Figure 6. The contribution of ozone concentration bins (incrementing in 10 ppb) to the M12 and PODy metric over the trend analysis period (2005–2021) for beech trees in EUR.

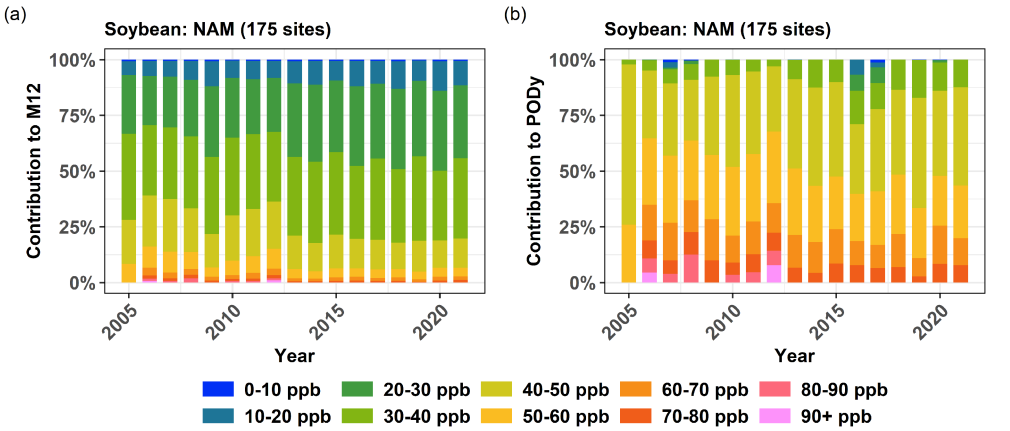

Figure 7. The contribution of ozone concentration bins (incrementing in 10 ppb) to the M12 and PODy metric over the trend analysis period (2005–2021) for soybean in NAM.

all years. This demonstrates the importance of the metrics '*y*' threshold of 6 nmol m^{-2} s^{-1} and a relatively low species specific g_{sto} (*gmax*) value of 300 mmol O_3 m^{-2} s^{-1}, which generally limits the contribution of lower ozone concentrations to the metric. However, the year 2016 shows that low ozone concentrations can, in exceptional circumstances, contribute to the PODy metric, probably owing to environmental conditions that would be favourable for g_{sto}.

(c) Ozone impacts

Following the methodology described in §S4 in the supplementary material, and using the DRRs listed in table S8 in the supplementary material, in combination with TOAR-II data from 2005 to 2021, we find that the larger estimated ozone effects on crops is a median relative yield loss (1-RYL) of 4.7% (10th and 90th percentiles: [0.2, 21.4]) for wheat (figure 8, boxplot RYL), with the most substantial relative yield losses in the Central USA, Southern and Western EUR (supplementary material, fig. S22b). By contrast, rice and soybean typically show negligible losses, with median RYL values of 0.3% ([0.0, 8.8]) and 0.0% ([0.0, 2.1]), respectively. Nonetheless, it should be noted that for rice, these results are based on sites with a very limited geographical distribution, located

Downloaded from royalsocietypublishing.org/rsta/article-pdf/doi/10.1098/rsta.2025.0270/6174187/rsta.2025.0270.pdf
by Univ. of Maryland user
on 30 October 2026

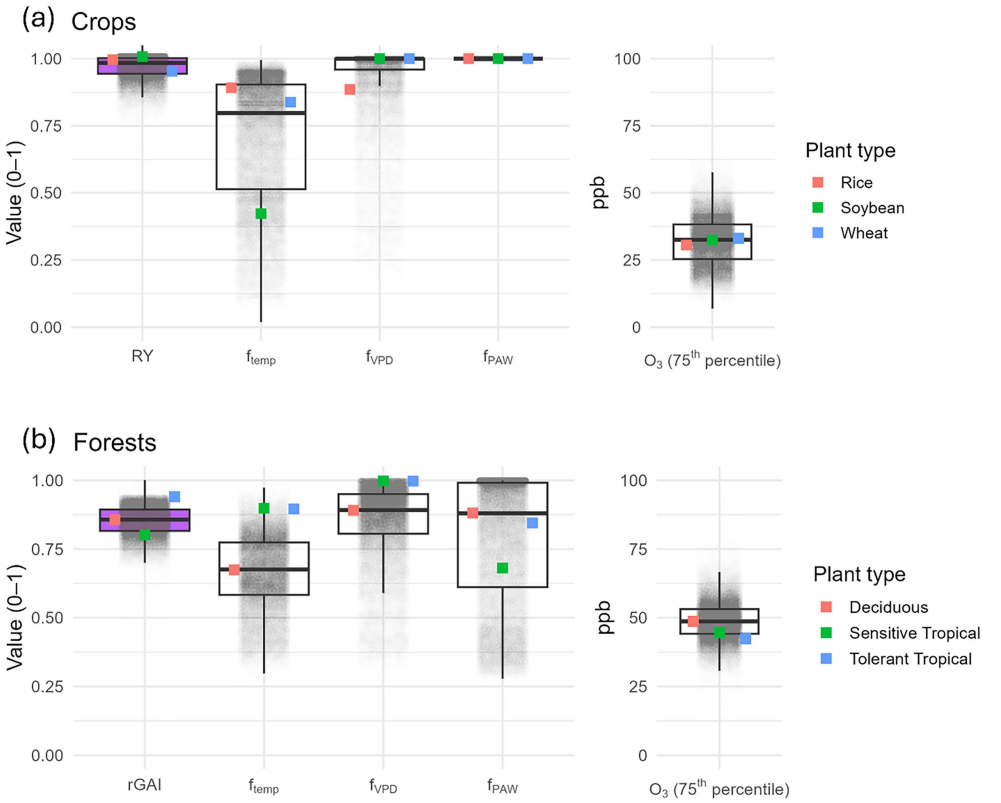

Figure 8. Boxplots with overlaid jittered points showing *ftemp*, *fVPD*, *fPAW*, *RYL/rGAI*, and the 75th percentile for ozone concentrations for crops (a) and forests (b). Coloured dots indicate the median values for each indicated plant type.

in the Republic of Korea and Northern Italy, which show an increased RYL (supplementary material, fig. S22d).

The main abiotic stressors that influence the ozone impact on vegetation are water stress, heat stress and decreased air humidity. These three factors contribute to g_{sto} reductions: (i) low soil water content owing to precipitation deficits or lack of irrigation (with soil water influence on g_{sto} denoted by f_{PAW}), (ii) high temperature (denoted by f_{temp}), and (iii) high leaf-to-air vapour pressure deficit (VPD) (denoted by f_{VPD}) can all reduce stomatal opening. Consequently, PODy is reduced, leading to a reduction of the negative effect of ozone on plant growth and production. Temperature seems to be the most limiting factor for all crops (figure 8a), and particularly for soybean, with g_{sto} reduced by 57.7% ([40.0, 79.0]); VPD exerts a substantial limiting effect only on rice (11.5% [2.6, 56.1]). The limiting effect of the plant's available water cannot be assessed because all the simulations were made assuming field capacity conditions. For wheat, the combined effect of temperature and VPD leads to increasing climatic limitations (see supplementary material, fig. S22a), particularly at higher latitudes in EUR and over the western NAM.

For trees, the loss of relative gross annual increment (1-*rGAI*) results in 14.3% [(8.3, 12.2)] for beech trees, 19.8% (8.1, 29.1) for sensitive tropical trees and 5.9% [(1.8, 9.1)] for tolerant tropical trees (figure 8b). The largest losses for beech trees are found in the Eastern NAM, and in Central EUR (supplementary material, fig. S22h). Temperature is a consistent limiting factor for beech (figure 8b) followed by the plant water availability in the soil, which also shows the largest variability; VPD is the least limiting factor. For the other tropical tree species, few sites are available for analysis, and therefore, their contribution to the total distribution of *rGAI* and the *f* functions are negligible. The climatic limitations roughly mirror the ozone effects, i.e. *rGAI* losses and climatic

Downloaded from royalsocietypublishing.org/rsta/article-pdf/doi/10.1098/rsta.2025.0270/6174187/rsta.2025.0270.pdf
by Univ. of Maryland user
on 30 October 2026

limitations are negatively correlated, revealing that the climate factors are the main driver of the spatial patterns of ozone stomatal uptake (supplementary material, fig. S22g,h).

4. Uncertainties in vegetation impact assessments

The approach to estimating uncertainty in modelled PODy is described in §S5 in the supplementary material. Figure 9 shows the distribution of the standard deviation of PODy (σPODy) for each land cover type derived from Monte Carlo simulations, which measure the statistical uncertainty of simulated PODy (associated with DO_3SE model parameters) and the ratio between mean σPODy and mean PODy (effects of systematic biases in key input variables (e.g. O_3) discussed later in this section). We find that the absolute values σPODy are generally larger over tree land cover types, where the threshold for PODy flux metrics y is lower (1 nmol O_3 m^{-2} PLA s^{-1} for trees versus 6 nmol O_3 m^{-2} PLA s^{-1} for crops; where PLA stands for projected leaf area), which leads to larger absolute values of PODy. However, after normalizing mean σPODy by mean PODy, we find that crops have much higher relative uncertainty in PODy (39% for wheat, 54% for rice and 72% for soybean) than trees (12% for sensitive tropical trees, 21% for tolerant tropical trees and 25% for beech trees). This indicates that the use of a higher y (the threshold above which ozone flux is considered to cause damage to the plant species and hence accumulated within the flux-based metric) could lead to larger relative uncertainty in simulated PODy (as the frequency of the ozone concentrations leading to an exceedance of a higher y will be lower owing to the ozone concentration distribution profile).

The distribution of Sobol sensitivity indices (SI) (which measures how much of the output variance is attributable to each variation of model parameters within their prescribed range) for each land cover type is shown in fig. S23 in the supplementary material. In general, we find that WebDO3SE-simulated PODy is most sensitive to (g_{max}), except the species specific maximum g_{sto} (g_{max}), except for beech and soybean, where the median SI to the temperature optimum for g_{sto} (T_{opt}) (around 0.4) is larger than that to g_{max}, while the median SI to the temperature minimum for g_{sto} (T_{min}) is also relatively high (0.21 for beech and 0.12 for soybean), indicating that PODy over these two land cover types is very sensitive to the parameters of the temperature limitation function. For most land cover types, PODy is not sensitive to parameters of the VPD limitation function, except for tolerant tropical forest and rice, where median SI to VPD minimum for g_{sto} (VPD_{min}) is greater than 0.1. Only two of the land cover types (tolerant tropical forest and rice) with the lowest *f_lightfrac* parameter (which determines the g_{sto} relationship to changing irradiance, f_{light}) show sensitivity of PODy (median SI > 0.1). PODy is also found to be less sensitive to the temperature maximum for g_{sto} (T_{max}) and the VPD maximum for g_{sto} (VPD_{max}) (median SI < 0.1 over all land types). This analysis identifies the most important model parameters, and potentially the ones that should be prioritized to constrain for different land cover types.

We also conduct specific input sensitivity tests to investigate the potential systematic errors of simulated PODy. First, we re-run the model with +25% and –25% ozone concentrations, which are representative of the range of error introduced by the vertical gradient of ozone (e.g. [45]), and the use of reanalysis data in regions without coverage of direct surface ozone measurements (i.e. Latin America, Africa—see §2c). The former is necessary as the ozone concentration measurement height is not detailed in the TOAR database. We also perform the following perturbation experiments: (i) growing season (by starting later by two weeks or ending earlier by two weeks), (ii) soil texture (by using the three additional soil texture classes available in webDO3SE), and (iii) root depth (+/– 0.5 m for temperate trees and 1 m for tropical trees).

The relative responses of land cover type-wide mean PODy to these perturbations are shown in fig. S24 in the supplementary material. We find that perturbing ozone concentration by 25% leads to a much stronger response in PODy for crops (–65% to +85% when ozone concentrations are reduced by 25%, and +89 to +191% when ozone concentrations are increased by 25%). By contrast, forest responses are within +/–31% to +/–36%, which is still greater than 25%. This indicates that errors in ozone can propagate nonlinearly to errors in simulated PODy, especially for land cover

Downloaded from royalsocietypublishing.org/rsta/article-pdf/doi/10.1098/rsta.2025.0270/6174187/rsta.2025.0270.pdf
by Univ. of Maryland user
on 30 October 2026

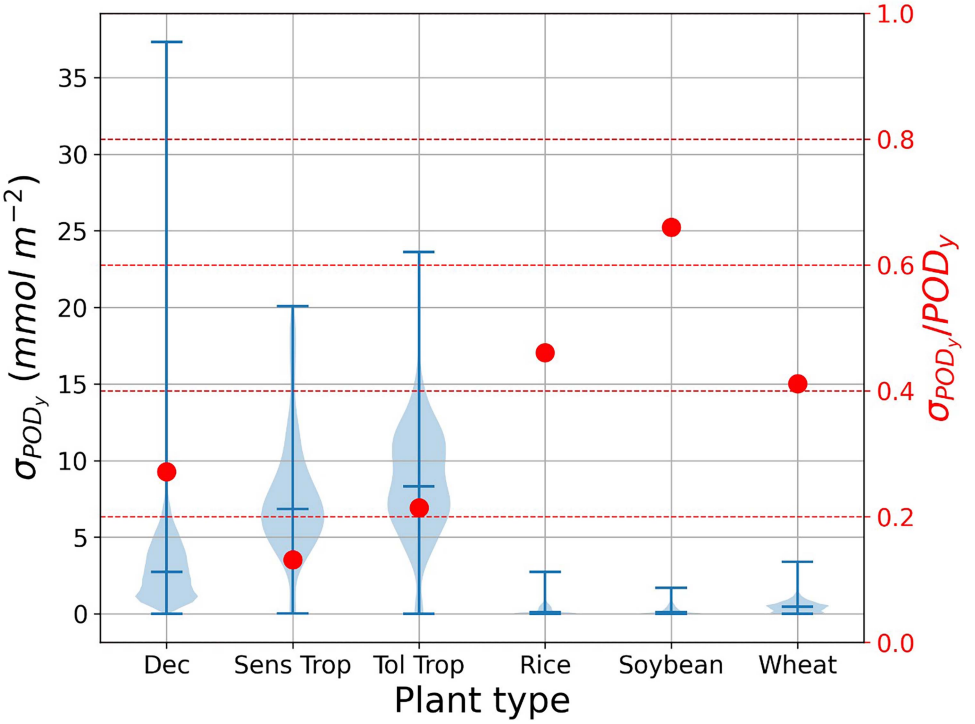

Figure 9. Distributions of standard deviation (σPODy, measure of statistical uncertainty) of PODy to DO3SE parameters for each land cover type. The red dots (scale corresponds to red y-axis) indicate the ratio between mean σPODy and mean PODy for each land cover type. The horizontal dashed lines indicate the minimum, median and maximum of each distribution.

types that have higher y thresholds. Shortening the growing season causes an up to 11% reduction in PODy for trees, as PODy accumulation happens over the whole growing season for trees. However, such effects on crops are much more uncertain (–26% to +14%), as PODy accumulation happens over a fixed period before the end of the growing season for crops, which only changes the timing, but not the length of the PODy accumulation period. Changing soil texture and root depth (which changes simulated soil water stress) leads to within 13% change in mean PODy over all forest types. For soil textures, simulated PODy increases as soil grain size decreases (from sandy loam to clay loam), as finer soil has better water retention, reducing simulated soil water stress. These results indicate that while the uncertainties in growing season and soil water stress simulation are not negligible, errors in ozone concentration generally have larger and nonlinear impacts on PODy, highlighting the importance of using more precise canopy-level ozone concentrations (e.g. through using measured ozone and performing proper measurement level to canopy scaling) in PODy estimations, especially when y thresholds are high. Finally, as simulated PODy and RYL for soybean are very low, we conducted an additional sensitivity simulation replacing T_{opt} with a value of 26°C after [46] and g_{max} with a value of 850 mmol O_3 PLA^{-1} m^{-2} s^{-1} after [37,47–50]. We find that mean simulated soybean PODy increased by almost tenfold, from 0.37 to 3.59 mmol m^{-2}. This highlights the importance of defining an appropriate g_{sto} parametrization for each land cover type.

5. Discussion

Overall, we find that 64% and 85% of sites exceed the critical levels for (wheat) crops and deciduous trees (beech) based on the AOT40 metric averaged over the period from 2016 to 2021. This compares with the previous TOAR-I vegetation assessment, which estimated AOT40 metric

Downloaded from royalsocietypublishing.org/rsta/article-pdf/doi/10.1098/rsta.2025.0270/6174187/rsta.2025.0270.pdf
by Univ. of Maryland user
on 30 October 2026

exceedance over the period from 2010 to 2014, using the same critical levels for crops (3 ppm h) and forests (5 ppm h) at 82.2% and 87.3% of sites, respectively [15]. The differences in the crop results may be owing to our use of different growing seasons, different site selection and a change in ozone concentrations since 2014. Our study also estimated PODy metric critical levels and found that 90% of sites for wheat and 79% of sites for beech showed exceedance. Therefore, there was reasonable agreement between metrics for deciduous trees (with 85% (for AOT40) and 79% (for PODy) of sites showing exceedance) but substantial differences for crops (where 64% (for AOT40) and 90% (for PODy) of sites showed exceedance for the 2016 to 2021 period). This suggests reasonable consistency in terms of metrics identifying sites where trees are at risk from ozone exposure, perhaps owing to the longer growing season smoothing out short-term differences in ozone exposure. For crops, the shorter growing seasons (especially for the PODy metric) may exacerbate differences in risk. The highest exceedance and hence suggested risk were found in the Western USA and Southern EUR for the M12, AOT40 and W126 metrics. This is also reasonably consistent with the previous TOAR-I vegetation assessment [15], which found overall the highest ozone values (mean, 2010–2014) to be in the mid-latitudes of the Northern Hemisphere, including Southern USA, the Mediterranean basin, North, North–West and East People's Republic of China. In this study, we also found that PODy presented a more evenly distributed risk across NAM, EUR and AS. Some key differences were in the west USA and East AS where lower risk was indicated for wheat and beech by the PODy than the concentration-based metrics.

In terms of global trends, for the period 2005–2021, we find that all metrics suggest similar trends for all species with more sites showing statistically significant decreasing trends with 30%, 14%, 39% and 40%, for M12, PODy, AOT40 and W126, respectively. By contrast, only 9%, 4%, 6% and 5% of sites have statistically significant increasing trends, respectively, by metric, the remaining sites showing no change. We also find that by region, metrics suggest a similar number of sites at which decreases in risk have occurred, although the PODy metric tends to estimate decreases at fewer sites than the concentration-based metrics.

The NAM region shows the greatest declines in ozone risk for all species (wheat, soybean, rice and beech), concentration-based metrics estimate between 56% to 66% of sites would see a decrease in risk, while PODy estimates only 23% of sites have a decreasing exposure over the 2005–2021 period. Split out into species, concentration-based metrics show decreasing trends for wheat at between 50% to 56% of sites, for rice between 48% to 55% of sites and for beech between 58% to 68% of sites. Findings for the concentration-based metrics are consistent with the previous TOAR-I vegetation assessment [15], which found that during 1995–2014, the dominant trend was a decrease in ozone at NAM sites; however, the number of sites at which decreasing trends were found differed with only 11% to 39% of sites seeing decreasing trends for wheat. Rice and perennial vegetation (the latter vegetation group similar to our studies beech) were more consistent but still estimated a higher number of sites (between 61% to 84% for rice and more than 70% of sites for beech) showing decreasing trends. By comparison, our study PODy estimates of sites with decreasing trends are substantially lower than the concentration-based metrics, with 40% for wheat, 21% for rice, 50% for soybean and 12% for beech.

In our study, EUR is the region with the next largest decreasing trend with between 10% and 16% of sites showing a reduction in ozone risk based on concentration-based metrics. By comparison, PODy estimates that only 7% of sites are moving towards lower ozone risk to vegetation. Again, split out into species groups, these trends for concentration-based metrics for wheat are between 1% to 12%, for rice between 14% to 22% and for beech between 11% to 17% of sites. By comparison, PODy estimates decreasing trends of 3% for wheat, 7% for rice, 2% for soybean and 12% for beech. The TOAR-I vegetation assessment [15] found that the number of EUR sites with decreasing trends was 17% to 32% for beech, 6% to 11% for wheat and 46% to 78% for rice, so overall, also lower than for NAM, and hence consistent with the relative findings of our study, even though a larger number of sites were found to have a decreasing trends. Both NAM (6% to 9% of sites) and EUR (1% to 7% of sites) have very few instances of increasing trends using concentration-based metrics; flux-based metrics show even more limited increasing trends, with only 1% of sites for both NAM and EUR.

Downloaded from royalsocietypublishing.org/rsta/article-pdf/doi/10.1098/rsta.2025.0270/6174187/rsta.2025.0270.pdf
by Univ. of Maryland user
on 30 October 2026

The AS region has the greatest complement of sites showing both trend directions with 16% to 29% of sites showing a decreasing trend with concentration-based metrics (and only 10% of sites decreasing with PODy); but also 18% to 29% of sites showing an increasing trend with concentration-based metrics, compared to 14% of sites in AS increasing when using PODy. This pattern was also reflected in the TOAR-I vegetation assessment [15] with the AS region showing a significant increase in the percentage of sites at ozone risk. However, our study results need to be interpreted with caution, given the limited spatial distribution of sites across East AS used in this analysis. Comparing between concentration-based metrics, W126 and AOT40 tend to estimate a greater percentage of sites with decreasing trends in ozone risk, while M12 tends to estimate more sites with increasing trends. This pattern holds for all three main regions and all three crops, as well as beech.

Although there is some variability in these results overall, they do show a general pattern of decreases in ozone metrics, which is greatest in NAM but also evident in EUR. These decreasing trends at NAM and EUR sites have been characterized by the shifting of high and low ozone levels towards the mid-range ozone levels [23], consistent with the implementation of large decreases in regional NOx emissions. Such trends are clearer for soybean (figure 7) than beech (figure 6) for both M12 and PODy metrics, suggesting that the averaging or accumulation period may be important in emphasizing changes in ozone concentration (given the shorter and more variable crop growing season). However, for both species, higher ozone levels declined, while lower ozone levels remained similar. This change in ozone concentration profile also helps to explain why the PODy metric does not always show the same magnitude of decreasing trend as found with the concentration-based metrics since decreases in higher ozone concentrations are counterbalanced by increases in more moderate ozone levels, which have greater influence on PODy than they do other concentration-based metrics. Similar results were found by Malley *et al.* [51] when comparing AOT40 and PODy metrics at two locations in the UK over a 23-year period (1990–2013) in relation to European NOx emission reductions.

The policy significance of these findings is important since regional policies that focus on NOx and volatile organic compound emission controls in EUR and NAM have been effective in reducing peak concentrations and exposure. This will probably result in greater improvements in concentration-based (especially those that emphasize higher ozone concentrations) than flux-based metrics. However, the growth in ozone precursor emissions elsewhere has increased the importance of background contributions to ozone worldwide. The effective controls for background ozone would be to reduce ozone precursors that operate at the hemispheric scale, particularly controls on methane, which should result in an overall decrease across the ozone concentration profile. Under such conditions, we might expect concentration-based metrics to show less improvement than the PODy metric, though this may depend upon how close the y threshold is to average ozone concentrations [1].

In addition to the assessment of risk and trends described above, this work has also estimated global relative yield losses for crops and relative gross annual increment losses for forest trees induced by ozone using the PODy ozone metric and available DRRs for the species studied. PODy was calculated using ozone concentration data from the TOAR database and the multiplicative g_{sto} model of WebDO3SE, driven by ERA5 meteorological data recently made available within the TOAR database, using parametrization obtained from the available literature. Our results estimate average RYLs of 4.7% for wheat across all sites studied. We find only relatively small losses for rice (0.3% on average), generally ranging between 0% and 8.8%, and negligible losses for soybean. This contrasts with a substantial body of literature identifying soybean as a highly ozone-sensitive crop, with reported yield reductions often around 10% to 15% or higher under current ozone levels (e.g. [33,52]). The magnitude of the impacts derived in our analysis is therefore unexpectedly low. Several factors may contribute to this inconsistency. First, differences in the ozone metrics used to relate ozone and damage strongly limit the direct comparability among studies. For example, the study of [33] primarily relied on cumulative exposure metrics modelled using a wheat parametrization to estimate PODy, but weighting the resulting wheat-yield loss estimates by the

Downloaded from royalsocietypublishing.org/rsta/article-pdf/doi/10.1098/rsta.2025.0270/6174187/rsta.2025.0270.pdf
by Univ. of Maryland user
on 30 October 2026

relative sensitivity of soybean, while [52] used a modelling approach based on ozone concentrations. However, it is well known that flux-based metrics such as PODy tend to reduce estimated impacts in situations where stomatal uptake is limited by environmental constraints, even under relatively high ambient ozone concentrations.

A second, and potentially more critical, source of uncertainty lies in the parametrization of the g_{sto} model adopted for soybean. This parametrization was based on the work of Zhang *et al.* [53], which, to our knowledge, represents the only published study providing a DRR for soybean based on POD_6 and supported by direct g_{sto} measurements over two consecutive growing seasons and across multiple cultivars. From this perspective, the selected parametrization is well justified. However, this parameter set includes a highly restrictive temperature response function, with an optimal temperature (T_{opt}) of 35°C. This value is unusually high when compared with values used for the other two crops considered in this study (26 and 28°C, for wheat and rice, respectively) and compared with soybean eco-physiological evidence reported elsewhere [46]. In addition, the g_{max} reported by Zhang *et al.* [53] is relatively low compared with values commonly found in the literature for soybean and with those reported in other studies [37,47–50]. Consequently, stomatal ozone uptake may be remarkably reduced under temperate conditions, leading to lower accumulated POD_6 values and, ultimately, to smaller damage estimates. This highlights the need for additional experimental datasets on soybean, including season-long g_{sto} measurements, yield responses and ozone levels.

For tropical trees, our parametrizations are based on the recent work of Cheesman *et al.* [54], which provides DRRs based on POD_1 for several different tropical species. However, the resulting relative gross annual increment relationships were based on only young trees, and with a fumigation period of only five months (while the growing season for these trees should typically be considered all-year round). These elements suggest that our results for soybean and tropical trees may be affected by the uncertainties in the g_{sto} parametrizations. This highlights the need for additional experimental datasets on these species, combining long-term g_{sto} measurements and DRRs, to better constrain PODy-based damage functions and reduce uncertainty in global-scale ozone impact assessments.

Notably, the different metrics used to assess vegetation impacts cover different time periods. This is particularly apparent for crops such as wheat, where the concentration-based metrics are over a three-month period, whereas for ozone uptake, the most sensitive six-week window is used. Although the shorter window is the most biologically relevant, this window can be difficult to identify at a global scale. Some crops have multiple growing seasons in a year, and the most productive growing season may or may not coincide with the highest ozone uptake. There can be changes in crop varieties at a single location over time, which may be able to adapt to a changing local climate or to a more productive variety. In addition to subtle changes to the timing of the growing season, there can be variation in ozone sensitivity of the different crop varieties, which has been shown for crops including African wheat [55], durum wheat [56] and soybean [57]. There can also be variations in the g_{sto} parametrization between different varieties, e.g. in wheat [58] which emphasize the importance of having g_{sto} parametrizations appropriate for the different agro–ecological regions for which flux-based metrics are applied [59].

Current air quality guidelines and standards vary between regions with many based on concentration-based metrics aiming to protect against adverse effects on human health [1,15]. Our study highlights the importance of flux-based metrics to assess trends and future predictions of ozone damage for vegetation. This will be increasingly important when assessing trends over longer time periods, because changes in climate will also need to be considered. The use of flux-based metrics may become more important in the future as only these metrics allow for the effects of climate-related variables (e.g. increased CO_2 as well as increased levels of drought and heat stress) in reducing g_{sto} and hence ozone uptake [60]. Other tools, such as crop models, are also now being developed that include ozone-damage functions; such modelling methods may supersede flux-based metrics in terms of assessing risk and damage since they are able to assess the combined effects of climate and ozone variables on yield (rather than simply incorporate the

Downloaded from royalsocietypublishing.org/rsta/article-pdf/doi/10.1098/rsta.2025.0270/6174187/rsta.2025.0270.pdf
by Univ. of Maryland user
on 30 October 2026

influence of climate on stomatal ozone uptake as is the case for current flux-based metrics) [61]. In cases where ozone damage and climate have been considered together, soil moisture and temperature have been identified as important modifying effects [52,62].

These findings have implications for several sustainable development goals. First, food security is likely to be affected by these ozone-induced yield losses. Our findings on a site-specific basis are corroborated with other global and regional modelling studies, using a variety of techniques, including the DRR risk assessment methods applied here, but also crop and land surface exchange modelling methods [61]. Current-day, global-scale assessments of crop damage using a variety of methodological approaches and a single, modelled ozone concentration field, found yield reductions for wheat, maize, soybean and rice of anywhere between 2.6% and 7.2% depending upon global region and choice of concentration or flux-based metric [19]. By comparison, a study using only flux-based metrics, again with a consistent ozone concentration field, found yield losses of between 4.4% and 12.4% [33]. These results are reasonably similar but do show the importance of modelled ozone concentrations (dependent upon emission estimates and atmospheric chemistry processes) as well as the selection of ozone-damage metrics. How changes in ozone concentration will affect future crop yields and food supply will depend not only on changes in emissions and consequent ozone concentrations, but also on climate change's influence on crop productivity and how this is managed. For example, irrigation is likely to become an even more important agricultural management tool as the climate heats, increasing water and heat stress over key agricultural regions. Studies have highlighted the role that ozone may play in limiting the productivity benefits of irrigation, especially for modern cultivars bred for high gas exchange [33,41]. Understanding the interplay between such key aspects of agricultural management and ozone will be important to understand future ozone impacts; arguably, this can most easily be done using either flux-based metrics or process-based modelling tools that incorporate physiological mechanisms that alter ozone uptake and decouple impacts from changes in ozone concentration alone. As such, including irrigation, using new and improved global datasets in future assessments of ozone damage will be important. Improving damage estimates becomes even more important given that ozone not only impacts yield quantity but also quality with new modelling studies showing promise in developing methods to estimate ozone-induced changes in protein yield related to amino acid nutritional indicators [8]. Second, in relation to climate action, modelling studies are beginning to develop more consistent agreement on the role that ozone might play in forest carbon sequestration, an important cost-effective, land-based climate mitigation approach [63]. A recent study [13] estimated that C sequestration to the living-biomass C stock of European forests would increase by 31% in the absence of ozone exposure. Such an increase in the yearly C sequestration to European C stocks (from –343 to –449 $MtCO_2$ eq yr^{-1}) has the potential to contribute substantially to the European Commission's action plan to develop sustainable solutions to increase C sequestration by forests. However, our study makes clear that improvements are needed to make reliable flux-based metric estimates and to use these with DRRs to assess actual damage.

Finally, our study goes some way towards informing us of the spatial and historical differences that exist between concentration and flux-based metrics. For those locations where TOAR database sites are at high density, this provides valuable information on the similarities or discrepancies between metrics and can help inform which metric, and for which species, would be most appropriate to use for vegetation-focused air quality management. Although our results generally show broad consistency between the concentration (M12) and flux-based metrics when applied to current and historic trends in data, the flux-based metrics are more biologically robust and are the recommended approach for future assessments as they would better account for any influence of climate change and alterations to vegetation physiology and phenology. However, our study also raises the issue of paucity of data, especially in AS where the limited distribution of available sites causes results to be inconclusive. Continued collation and analysis of data in a TOAR-III effort could make important inroads into improving our understanding of ozone impacts and their trends in this (and other regions) in the future.

Downloaded from royalsocietypublishing.org/rsta/article-pdf/doi/10.1098/rsta.2025.0270/6174187/rsta.2025.0270.pdf
by Univ. of Maryland user
on 30 October 2026

Priorities for a third phase to improve assessments of ozone impacts to vegetation would be: (i) increase the number of TOAR database sites in AS, Africa and Latin America, (ii) develop g_{sto} model parametrizations for agro-ecological regions, and (iii) develop flux-based DRRs for crop and forest tree species, especially tropical species. If successful, these efforts would see a step change in our understanding of the impacts of ozone at a global scale and how these impacts have changed over time, helping to inform future risk, mitigation and adaptation options.

Ethics. This work did not require ethical approval from a human subject or animal welfare committee.

Data accessibility. The data and codes presented in this manuscript are publicly available on the Zenodo repository under the permanent identifier [64].

Supplementary material is available online [65].

Declaration of AI use. We have not used AI-assisted technologies in creating this article.

Author's contributions. L.E.: conceptualization, formal analysis, investigation, methodology, supervision, writing—original draft; T.E.: conceptualization, data curation, formal analysis, methodology, writing—original draft; P.G.: formal analysis, investigation, methodology, visualization, writing—original draft; A.A.M.: conceptualization, formal analysis, investigation, methodology, writing—original draft; F.H.: conceptualization, formal analysis, investigation, methodology, writing—original draft; S.S.: conceptualization, data curation, formal analysis, methodology, writing—original draft; A.Y.H.W.: investigation, methodology, writing—original draft; N.B.: formal analysis; R.M.: investigation, methodology; G.G.: conceptualization, formal analysis, methodology, writing—original draft; M.S.: conceptualization, methodology; M.H.: writing—original draft; L.Z.: conceptualization.

All authors gave final approval for publication and agreed to be held accountable for the work performed therein.

Conflict of interest declaration. We declare we have no competing interests.

Funding. No funding has been received for this article.

Acknowledgements. The authors gratefully acknowledge the Gauss Centre for Supercomputing e.V. (www.gauss-centre.eu) for providing computing time and storage on the GCS Supercomputer JUWELS. T.E. thanks the German Research Foundation as part of the CLICCS Clusters of Excellence (DFG EXC 2037).

References

1. Emberson L. 2020 Effects of ozone on agriculture, forests and grasslands. *Phil. Trans. R. Soc. A* **378**, 20190327. (doi:10.1098/rsta.2019.0327)
2. Moura BB, Alves ES, de Souza SR, Domingos M, Vollenweider P. 2014 Ozone phytotoxic potential with regard to fragments of the Atlantic semi-deciduous forest downwind of Sao Paulo, Brazil. *Environ. Pollut.* **192**, 65–73. (doi:10.1016/j.envpol.2014.05.014)
3. Ueno AC, Gundel PE, Ghersa CM, Agathokleous E, Martínez-Ghersa MA. 2021 Seed-borne fungal endophytes constrain reproductive success of host plants under ozone pollution. *Environ. Res.* **202**, 111773. (doi:10.1016/j.envres.2021.111773)
4. Fuhrer J. 2009 Ozone risk for crops and pastures in present and future climates. *Naturwissenschaften* **96**, 173–194. (doi:10.1007/s00114-008-0468-7)
5. Ainsworth EA. 2017 Understanding and improving global crop response to ozone pollution. *Plant J.* **90**, 886–897. (doi:10.1111/tpj.13298)
6. Feng Z, Kobayashi K. 2009 Assessing the impacts of current and future concentrations of surface ozone on crop yield with meta-analysis. *Atmos. Environ.* **43**, 1510–1519. (doi:10.1016/j.atmosenv.2008.11.033)
7. Broberg MC, Feng Z, Xin Y, Pleijel H. 2015 Ozone effects on wheat grain quality – a summary. *Environ. Pollut.* **197**, 203–213. (doi:10.1016/j.envpol.2014.12.009)
8. Cook J, Yadav DS, Hayes F, Booth N, Bland S, Pande P, Thankappan S, Emberson L. 2025 Modelling ozone-induced changes in wheat amino acids and protein quality using a process-based crop model. *Biogeosciences* **22**, 1035–1056. (doi:10.5194/bg-22-1035-2025)
9. Pandey D *et al.* 2023 Assessing the costs of ozone pollution in India for wheat producers, consumers, and government food welfare policies. *Proc. Natl Acad. Sci. USA* **120**, e2207081120. (doi:10.1073/pnas.2207081120)

Downloaded from royalsocietypublishing.org/rsta/article-pdf/doi/10.1098/rsta.2025.0270/6174187/rsta.2025.0270.pdf
by Univ. of Maryland user
on 30 October 2026

10. Grulke NE, Heath RL. 2020 Ozone effects on plants in natural ecosystems. *Plant Biol. J.* **22**, 12–37. (doi:10.1111/plb.12971)
11. Fuhrer J, Val Martin M, Mills G, Heald CL, Harmens H, Hayes F, Sharps K, Bender J, Ashmore MR. 2016 Current and future ozone risks to global terrestrial biodiversity and ecosystem processes. *Ecol. Evol.* **6**, 8785–8799. (doi:10.1002/ece3.2568)
12. Koike T, Watanabe M, Hoshika Y, Kitao M, Matsumura H, Funada R, Izuta T. 2013 Effects of ozone on forest ecosystems in East and Southeast Asia. In *Climate change, air pollution and global challenges: understanding and perspectives from forest research*, (eds R Matyssek, N Clarke, P Cudlin, TN Mikkelsen, J-P Tuovinen, G Wieser, E Paoletti), pp. 371–390. Amsterdam, The Netherlands: Elsevier.
13. Karlsson PE, Büker P, Bland S, Simpson D, Sharps K, Hayes F, Emberson LD. 2025 Ozone causes substantial reductions in the carbon sequestration of managed European forests. *Biogeosciences* **22**, 3563–3582. (doi:10.5194/bg-22-3563-2025)
14. Cheesman AW *et al.* 2024 Reduced productivity and carbon drawdown of tropical forests from ground-level ozone exposure. *Nat. Geosci.* **17**, 1003–1007. (doi:10.1038/s41561-024-01530-1)
15. Mills G *et al.* 2018 Tropospheric Ozone Assessment Report: present-day tropospheric ozone distribution and trends relevant to vegetation. *Elementa* **6**, 47. (doi:10.1525/elementa.302)
16. Pleijel H, Danielsson H, Broberg MC. 2022 Benefits of the phytotoxic ozone dose (POD) index in dose-response functions for wheat yield loss. *Atmos. Environ.* **268**, 118797. (doi:10.1016/j.atmosenv.2021.118797)
17. Mills G *et al.* 2011 New stomatal flux-based critical levels for ozone effects on vegetation. *Atmos. Environ.* **45**, 5064–5068. (doi:10.1016/j.atmosenv.2011.06.009)
18. Hayes F, Harmens H, Mills G, Bender J, Grünhage L. 2020 Ozone critical levels for (semi-)natural vegetation dominated by perennial grassland species. *Environ. Sci. Pollut. Res.* **28**, 15 090–15 098. (doi:10.1007/s11356-020-11724-w)
19. Tai APK, Sadiq M, Pang JYS, Yung DHY, Feng Z. 2021 Impacts of surface ozone pollution on global crop yields: comparing different ozone exposure metrics and incorporating co-effects of CO_2. *Front. Sustain. Food Syst.* **5**, 534616. (doi:10.3389/fsufs.2021.534616)
20. Mills G, Hayes F, Simpson D, Emberson L, Norris D, Harmens H, Büker P. 2011 Evidence of widespread effects of ozone on crops and (semi-)natural vegetation in Europe (1990–2006) in relation to AOT40- and flux-based risk maps. *Glob. Chang. Biol.* **17**, 592–613. (doi:10.1111/j.1365-2486.2010.02217.x)
21. Karlsson PE *et al.* 2007 Risk assessments for forest trees: the performance of the ozone flux versus the AOT concepts. *Environ. Pollut.* **146**, 608–616. (doi:10.1016/j.envpol.2006.06.012)
22. Mills G *et al.* 2018 Ozone pollution will compromise efforts to increase global wheat production. *Glob. Chang. Biol.* **24**, 3560–3574. (doi:10.1111/gcb.14157)
23. Lefohn AS *et al.* 2018 Tropospheric Ozone Assessment Report: global ozone metrics for climate change, human health, and crop/ecosystem research. *Elementa* **6**, 27. (doi:10.1525/elementa.279)
24. Emmerichs T *et al.* 2025 Can atmospheric chemistry deposition schemes reliably simulate stomatal ozone flux across global land covers and climates? *Biogeosciences* **22**, 4823–4849. (doi:10.5194/bg-22-4823-2025)
25. Clifton OE *et al.* 2023 A single-point modeling approach for the intercomparison and evaluation of ozone dry deposition across chemical transport models (Activity 2 of AQMEII4). *Atmos. Chem. Phys.* **23**, 9911–9961. (doi:10.5194/acp-23-9911-2023)
26. Emberson LD, Ashmore MR, Cambridge HM, Simpson D, Tuovinen J-P. 2000 Modelling stomatal ozone flux across Europe. *Environ. Pollut.* **109**, 403–413. (doi:10.1016/s0269-7491(00)00043-9)
27. Büker P *et al.* 2012 DO_3SE modelling of soil moisture to determine ozone flux to forest trees. *Atmos. Chem. Phys.* **12**, 5537–5562. (doi:10.5194/acp-12-5537-2012)
28. Simpson D *et al.* 2012 The EMEP MSC-W chemical transport model – technical description. *Atmos. Chem. Phys.* **12**, 7825–7865. (doi:10.5194/acp-12-7825-2012)
29. Tuovinen J-P, Emberson L, Simpson D. 2009 Modelling ozone fluxes to forests for risk assessment: status and prospects. *Ann. For. Sci.* **66**, 401. (doi:10.1051/forest/2009024)
30. Schultz MG *et al.* 2017 Tropospheric Ozone Assessment Report: database and metrics data of global surface ozone observations. *Elementa* **5**, 58. (doi:10.1525/elementa.244)

Downloaded from royalsocietypublishing.org/rsta/article-pdf/doi/10.1098/rsta.2025.0270/6174187/rsta.2025.0270.pdf
by Univ. of Maryland user
on 30 October 2026

31. Tarasick DW *et al.* 2019 Quantifying stratosphere-troposphere transport of ozone using balloon-borne ozonesondes, radar windprofilers and trajectory models. *Atmos. Environ.* **198**, 496–509. (doi:10.1016/j.atmosenv.2018.10.040)
32. FAOSTAT. 2025 *FAOSTAT Crop and livestock products*. https://www.fao.org/faostat/en/}data/QCL.
33. Mills G *et al.* 2018 Closing the global ozone yield gap: quantification and cobenefits for multistress tolerance. *Glob. Chang. Biol.* **24**, 4869–4893. (doi:10.1111/gcb.14381)
34. Osborne SA, Mills G, Hayes F, Ainsworth EA, Büker P, Emberson L. 2016 Has the sensitivity of soybean cultivars to ozone pollution increased with time? An analysis of published dose–response data. *Glob. Chang. Biol.* **22**, 3097–3111. (doi:10.1111/gcb.13318)
35. Büker P *et al.* 2015 New flux based dose–response relationships for ozone for European forest tree species. *Environ. Pollut.* **206**, 163–174. (doi:10.1016/j.envpol.2015.06.033)
36. Li P, Feng Z, Catalayud V, Yuan X, Xu Y, Paoletti E. 2017 A meta-analysis on growth, physiological, and biochemical responses of woody species to ground-level ozone highlights the role of plant functional types. *Plant Cell Environ.* **40**, 2369–2380. (doi:10.1111/pce.13043)
37. CLRTAP. 2017 Mapping critical levels for vegetation, chapter III. In *Manual on methodologies and criteria for modelling and mapping critical loads and levels and air pollution effects, risks and trends*. Geneva, Switzerland: UNECE.
38. Fischer G, van Velthuizen H. *Global Agro-ecological zones v3.0*. http://www.gaez.iiasa.ac.at/ (accessed 01 December 2015).
39. Jägermeyr J, Müller C, Minoli S, Ray D, Siebert S. 2021 GGCMI phase 3 crop calendar. Zenodo. (doi:10.5281/zenodo.5062513)
40. Soci C *et al.* 2024 The ERA5 global reanalysis from 1940 to 2022. *Q. J. R. Meteorol. Soc.* **150**, 4014–4048. (doi:10.1002/qj.4803)
41. Everett G *et al.* 2025 Ozone pollution may limit the benefits of irrigation to wheat productivity in India. *Biogeosciences* **22**, 4203–4219. (doi:10.5194/bg-22-4203-2025)
42. Meier J, Zabel F, Mauser W. 2018 A global approach to estimate irrigated areas – a comparison between different data and statistics. *Hydrol. Earth Syst. Sci.* **22**, 1119–1133. (doi:10.5194/hess-22-1119-2018)
43. Miyazaki K *et al.* 2020 Updated tropospheric chemistry reanalysis and emission estimates, TCR-2, for 2005–2018. *Earth Syst. Sci. Data* **12**, 2223–2259. (doi:10.5194/essd-12-2223-2020)
44. Jones DBA *et al.* 2025 *Supplementary material to "Assessment of regional and interannual variations in tropospheric ozone in chemical reanalyses"*. https://egusphere.copernicus.org/preprints/2025/egusphere-2024-3759/egusphere-2024-3759-supplement.pdf.
45. Gerosa G, Marzuoli R, Monteleone B, Chiesa M, Finco A. 2017 Vertical ozone gradients above forests. Comparison of different calculation options with direct ozone measurements above a mature forest and consequences for ozone risk assessment. *Forests* **8**, 337. (doi:10.3390/f8090337)
46. Jumrani K, Bhatia VS, Pandey GP. 2017 Impact of elevated temperatures on specific leaf weight, stomatal density, photosynthesis and chlorophyll fluorescence in soybean. *Photosynth. Res.* **131**, 333–350. (doi:10.1007/s11120-016-0326-y)
47. Bou Jaudé M, Katerji N, Mastrorilli M, Rana G. 2008 Analysis of the effect of ozone on soybean in the Mediterranean region: I. The consequences on crop-water status. *Eur. J. Agron.* **28**, 508–518. (doi:10.1016/j.eja.2007.09.002)
48. Gillespie KM, Xu F, Richter KT, McGrath JM, Markelz RJC, Ort DR, Leakey ADB, Ainsworth EA. 2012 Greater antioxidant and respiratory metabolism in field-grown soybean exposed to elevated O_3 under both ambient and elevated CO_2. *Plant Cell Environ.* **35**, 169–184. (doi:10.1111/j.1365-3040.2011.02427.x)
49. Gilbert ME, Holbrook NM, Zwieniecki MA, Sadok W, Sinclair TR. 2011 Field confirmation of genetic variation in soybean transpiration response to vapor pressure deficit and photosynthetic compensation. *Field Crops Res.* **124**, 85–92. (doi:10.1016/j.fcr.2011.06.011)
50. Betzelberger AM, Yendrek CR, Sun J, Leisner CP, Nelson RL, Ort DR, Ainsworth EA. 2012 Ozone exposure response for U.S. soybean cultivars: linear reductions in photosynthetic potential, biomass, and yield. *Plant Physiol.* **160**, 1827–1839. (doi:10.1104/pp.112.205591)
51. Malley CS, Heal MR, Mills G, Braban CF. 2015 Trends and drivers of ozone human health and vegetation impact metrics from UK EMEP supersite measurements (1990–2013). *Atmos. Chem. Phys.* **15**, 4025–4042. (doi:10.5194/acp-15-4025-2015)

Downloaded from royalsocietypublishing.org/rsta/article-pdf/doi/10.1098/rsta.2025.0270/6174187/rsta.2025.0270.pdf
by Univ. of Maryland user
on 30 October 2026

52. Schauberger B, Rolinski S, Schaphoff S, Müller C. 2019 Global historical soybean and wheat yield loss estimates from ozone pollution considering water and temperature as modifying effects. *Agric. For. Meteorol.* **265**, 1–15. (doi:10.1016/j.agrformet.2018.11.004)
53. Zhang J, Tang H, Liu G, Zhu JG. 2016 Stomatal ozone flux-response relationships of rice (oryza sativa L.) in subtropical area. *J. Agro-Environ. Sci.* **35**, 1857–1866. (doi:10.11654/jaes.2016-0594)
54. Cheesman AW *et al.* 2023 Impacts of ground-level ozone on sugarcane production. *Sci. Total Environ.* **904**, 166817. (doi:10.1016/j.scitotenv.2023.166817)
55. Hayes F, Sharps K, Harmens H, Roberts I, Mills G. 2020 Tropospheric ozone pollution reduces the yield of African crops. *J. Agron. Crop Sci.* **206**, 214–228. (doi:10.1111/jac.12376)
56. Monga R, Marzuoli R, Alonso R, Bermejo V, González-Fernández I, Faoro F, Gerosa G. 2015 Varietal screening of ozone sensitivity in Mediterranean durum wheat (*Triticum durum*, Desf.). *Atmos. Environ.* **110**, 18–26. (doi:10.1016/j.atmosenv.2015.03.040)
57. Jiang L, Feng Z, Dai L, Shang B, Paoletti E. 2018 Large variability in ambient ozone sensitivity across 19 ethylenediurea-treated Chinese cultivars of soybean is driven by total ascorbate. *J. Environ. Sci.* **64**, 10–22. (doi:10.1016/j.jes.2017.07.002)
58. Feng Y, Nguyen TH, Alam MS, Emberson L, Gaiser T, Ewert F, Frei M. 2022 Identifying and modelling key physiological traits that confer tolerance or sensitivity to ozone in winter wheat. *Environ. Pollut.* **304**, 119251. (doi:10.1016/j.envpol.2022.119251)
59. Pande P, Bland S, Booth N, Cook J, Feng Z, Emberson L. 2025 Development of the DO_3SE-crop model to assess ozone effects on crop phenology, biomass, and yield. *Biogeosciences* **22**, 181–212. (doi:10.5194/bg-22-181-2025)
60. Sillmann J, Aunan K, Emberson L, Büker P, Van Oort B, O'Neill C, Otero N, Pandey D, Brisebois A. 2021 Combined impacts of climate and air pollution on human health and agricultural productivity. *Environ. Res. Lett.* **16**, 093004. (doi:10.1088/1748-9326/ac1df8)
61. Emberson LD *et al.* 2018 Ozone effects on crops and consideration in crop models. *Eur. J. Agron.* **100**, 19–34. (doi:10.1016/j.eja.2018.06.002)
62. Nguyen TH *et al.* 2024 Assessing the spatio-temporal tropospheric ozone and drought impacts on leaf growth and grain yield of wheat across Europe through crop modeling and remote sensing data. *Eur. J. Agron.* **153**, 127052. (doi:10.1016/j.eja.2023.127052)
63. Griscom BW *et al.* 2017 Natural climate solutions. *Proc. Natl Acad. Sci. USA* **114**, 11 645–11 650. (doi:10.1073/pnas.1710465114)
64. Emberson L *et al.* 2026 codes and data for Tropospheric Ozone Assessment Report II: Analysis of global ozone distribution and trends to assess vegetation impacts (Version 1.0.0) [Dataset]. Zenodo. (doi:10.5281/zenodo.20283591)
65. Emberson L *et al.* 2026 Supplementary material from: Tropospheric Ozone Assessment Report II: Analysis of global ozone distribution and trends to assess vegetation impacts. Figshare. (doi:10.6084/m9.figshare.c.8631039)

Downloaded from royalsocietypublishing.org/rsta/article-pdf/doi/10.1098/rsta.2025.0270/6174187/rsta.2025.0270.pdf
by Univ. of Maryland user
on 30 October 2026